Arabian Journal of Chemistry (2017) **10**, S3338–S3346

King Saud University

Arabian Journal of Chemistry

www.ksu.edu.sa
www.sciencedirect.com

ORIGINAL ARTICLE

Reactivity trends of hydroxide ion attack on high spin Fe(II) complexes including bromosalicylidene amino acid ligands in some mixed aqueous solvents: Gibb's Free Energy of Transfer and initial-transition state analysis

Laila H. Abdel-Rahman, Rafat M. El-Khatib, Lobna A.E. Nassr, Ahmed M. Abu-Dief *

Chemistry Department, Faculty of Science, Sohag University, 82534 Sohag, Egypt

Received 6 August 2013; accepted 21 January 2014
Available online 1 February 2014

KEYWORDS

Base hydrolysis;
Kinetics;
Solvolysis;
Chelate;
Gibb's Free Energy of Transfer;
Initial state-transition state

Abstract The kinetics of hydroxide ion attack on bis(bromosalicylidene alanate)iron (II) (bsali), bis(bromosalicylidene phenylalanate)iron(II) (bsphali), bis(bromosalicylidene aspartate)iron(II) (bsasi), (bromosalicylidene histidinate)iron(II) (bshi), bis(bromosalicylidene arginate)iron(II) (bsari) have been reported in different binary aqueous solvent mixtures at 298 K. The observed reactivity trends are discussed in terms of the hydrophilic and hydrophobic forms of the complexes investigated, as well as the transfer chemical potentials of hydroxide ion and the complex. Both the solvent–solute and solvent–solvent interactions have been considered. The hydrophobic character of the complexes studied was manifested by decreasing in reactivity. Solvent effect on reactivity trends of the investigated complexes has been analyzed into initial and transition state components by using the transfer chemical potentials of the reactants and the kinetic data of the studied compounds. The decrease in the observed rate constant values (k_{obs}) of the base hydrolysis of the investigated complexes with increasing of solvent % is dominated by the initial state (IS).

1. Introduction

1.1. Application of Schiff base amino acid complexes

From a bioinorganic point of view, iron Schiff base complexes provide useful structural and electronic models for the similarly coordinated sites found in the heme iron enzymes. Moreover, these complexes are also important for the asymmetric oxidation of organic substrates, since their

* Corresponding author. Tel.: +20 934601807/2556; mobile: +20 164162700; fax: +20 934601159.
E-mail address: ahmed_benzoic@yahoo.com (A.M. Abu-Dief).
Peer review under responsibility of King Saud University.

Production and hosting by Elsevier

http://dx.doi.org/10.1016/j.arabjc.2014.01.013
1878-5352

structure and catalytic activity are analogous with those of iron porphyrins (Canali and Sherrington, 1999). Schiff base amino acid complexes act as good chelating agents (Nath and Yadov, 1997; Abdel-Rahman et al., 2014) and behave as efficient biologically active (Abdel-Rahman et al., 2013; El-Said et al., 2001) and cytotoxic (Wang et al., 2002) agents. In addition, Schiff base amino acid complexes are considered to constitute new kinds of potential antibacterial and anticancer reagents (Wang et al., 2005).

1.2. Medium effects on reactivity

The effects of both solvents upon a variety of reactions of transition metal complexes have been of interest in recent years. Most reactions of inorganic complexes exhibit different reactivities in micellar and microemulsion systems from those in aqueous solutions. Thus, the appropriate use of microemulsions can allow kinetic studies to be made of reactions involving either water-insoluble reactants or, in some cases, such Schiff base amino acid complexes, hydrophobic substrates (Burgess and Pelizzetti, 1988; Burgess and Pelizzetti, 1992). More recently, trends in transfer chemical potentials and their relation to reactivity trends for substitution and redox reactions of these inorganic complexes have been investigated in binary aqueous mixtures (Blandamer et al., 1988). Furthermore, a new approach to understanding solvent effects on reaction rates involves consideration of the extent of the interaction of the solvent environments of the initial state and the transition state with the solvent co sphere of an added substance (Milde et al., 1999). Most treatments of solvent effects on reactivity deal with the rate constant and activation parameter trends, but others have recognized that such kinetic parameters are composite values. Analysis of solvent effects on reactivities in terms of the contributions from the initial and transition states can lead to full explanations of these trends (Burgess and Pelizzetti, 1988; Burgess and Pelizzetti, 1992; Abu-Gharib et al., 2011). In parallel with these trends, solvation effects can be probed via the variation of activation volume with the properties of the solvent (Bähr and Döge, 1957). These two approaches are complementary in that analysis of the initial and transition states provides information on solvation changes for a reaction involved in a suggested mechanism on transfer from one medium to another, whereas knowledge of the activation volume can test solvation changes on going from the initial to the transition state in a specific medium (Yamagishi, 1986; Abu-Gharib et al., 2011; Abu-Gharib et al., 2017). It is worthy to recall that thermodynamic functions, e.g., solubility, provide information on transfer of the initial state, whereas solvent effects on the transition state can be derived from these measurements and the observed rate constants (Bähr and Döge, 1957). In the present contribution, we present an extensive investigation of these approaches through the study of solvent effects on the reactivity of the base hydrolysis of a new series of hydrophobic high-spin iron(II) amino acid Schiff base chelates. Moreover, the effect of solvent on reactivity trends has been analyzed into initial and transition state analysis to give an overall idea about the role of solvent in the reactivity.

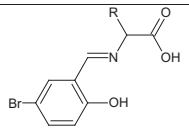

Acronym		R
Ligand	**Complex**	
bsal	bsali	CH_3
bsphal	bsphali	$CH_2C_6H_5$
bsas	bsasi	CH_2COOH
bsh	bshi	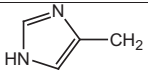
bsar	bsari	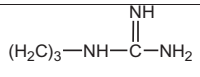

Scheme 1 Structures and abbreviations of the Schiff base ligands and abbreviations of their corresponding complexes.

2. Experimental

2.1. Preparation of the investigated complexes

The solid Schiff base amino acid Fe(II) complexes were prepared by mixing aqueous solutions of the respective amino acids [L-Alanine (ala), L-Phenylalanine (phala), L-Aspartic acid (asp), L-Histidine (his) and L-Arginine (arg)] with an equimolar hot ethanolic solution of 5-bromosalicyaldhyde (BrSal). The resulting Schiff base amino acid ligands (the ligands are displayed and labeled in Scheme 1) were then treated with an aqueous solution of ferrous ammonium sulfate in an equimolar ratio. In order to avoid the oxidation of Fe(II) and the formation of $Fe(OH)_3$, a few drops of glacial acetic acid were added (Sharma and Dubey, 1994; Abdel-Rahman et al., 2013, 2014; Blandamer et al., 1992). The resulting solution was stirred for 8 h under nitrogen. The precipitated complexes were filtered off, washed with a water–ethanol mixture, and then with diethyl ether. The complexes were first dried on a water bath and then in vacuo over P_2O_5. The isolated complexes were crystallized from water–ethanol solutions (Abdel-Rahman et al., 2014). The composition of the complexes was established by CHN microanalysis, IR, and UV/vis spectral analyses. All gave satisfactory CHN microanalysis (Abdel-Rahman et al., 2014). The stability of solutions was tested for at least a month for evidence of oxidation of the Fe(II) cation by peroxopersulfate or reduction by dithionite. When the aged complex solutions were treated with NaOH under nitrogen, a green precipitate of $Fe(OH)_2$ formed, indicating the maintenance of Fe(II) oxidation state in the complex solutions used in the kinetic runs. It was observed that, in these runs, the intensely violet color of the complex fades and the solution turns colorless. Some green colloidal particles of $Fe(OH)_2$ form initially, turning pale yellow, and, finally, precipitating as brown $Fe(OH)_3$ by oxidation with O_2 dissolved in solution kept long after end of the kinetic run. Full details of the characterization of the present complexes can be found in our previous publication (Abdel-Rahman et al., 2014).

2.2. Kinetics

Kinetic measurements were carried out spectrophotometrically by following the decrease in absorbance with time at λ_{max} in the UV–vis region appropriate to each complex (see Scheme 2). The kinetic data were recorded using PG UV–Visible spectrophotometer model T + 80 with 10 mm matched quartz cells connected with an ultrathermostate (CRIOTERM model 190) water circulator. The reactants were brought together so that the reaction exhibits pseudo-first order kinetics by mixing a multifold greater concentration of the base than that of the complex. It was confirmed that there is no interference from other reagents at the selected wavelength absorption maxima for the investigated complexes. Rate constants were calculated from the dependence of absorbance on time at λ_{max} for the base hydrolysis of each complex. Each experiment was duplicated to ensure satisfactory reproducibility of the kinetic parameters (Bähr and Thämlitz, 1955) (see Scheme 3).

2.3. Solubilities

Solubilities were measured at 298 K ± 0.1 K by agitating a generous excess of each complex with the appropriate water–ethanol, water–acetone, water–propanol and water–dimethyl sulfoxide mixtures in a thermostated vessel for 7 h. This time is enough to prepare the best saturated solution from the solid compound in aqueous-solvent mixtures. Then portions of supernatant saturated solution were removed and centrifuged rapidly using centrifuge before withdrawing an aliquot by using a micropipette. The solution was diluted as necessary. Then the absorbance was measured at λ_{max} for each complex (Bähr and Thämlitz, 1955; Blandamer et al., 1986). All aliquots of equilibrated solutions were diluted with the solvent and the dependences of λ_{max} on solvent composition, were found to be very small for the studied complexes, and thus ignored in calculation of solubilities. The customary precautions were taken to avoid heating of aliquots of saturated solutions before dilution and to prevent any solid material being carried through with samples of saturated solutions. The spectra were measured at different sampling times to verify that a constant concentration has been achieved. The concentrations of the saturated solutions were determined by applying beer's law (A_{abs} = εcl) where "ε" is the molar extension coefficient in $dm^3\ mol^{-1}\ cm^{-1}$, "c" is the concentration in mol dm^{-3} and "l" is the length of the cell in cm. The molar extension coefficient "ε" in $dm^3\ mole^{-1}\ cm^{-1}$ for each complex was determined from the least square of the standard curve using beer's law.

3. Results and discussion

3.1. Kinetic results and reaction mechanism

The fading of color of the solutions of the Fe(II) amino acid Schiff base complexes by hydroxide ion indicates that the complete dissociation occurs. In the presence of excess hydroxide ion and oxygen, the ultimate product, in addition to the ligand, is $Fe(OH)_3$. The overall rate law for the investigated reaction under the adopted conditions of pseudo first order kinetics can be represented as follows:

$$\text{Rate} = k_{obs}[\text{complex}] = (k_1 + k_2[OH^-])[\text{complex}] \quad (1)$$

The k_1 term is assigned to rate determining dissociation of the investigated complexes and the k_2 term to rate determining attack by OH^- at the compounds, where $k_{obs} = k_1 + k_2$ [OH]. The values of the rate constants for the base hydrolysis reaction of the investigated complexes in aqueous solution are shown in Tables 1 and 3. The first hydroxide ion adds to the electrophilic carbonium of the polarized azomethine in a fast pre-equilibrium step, as was reported by Mahmoud et al.

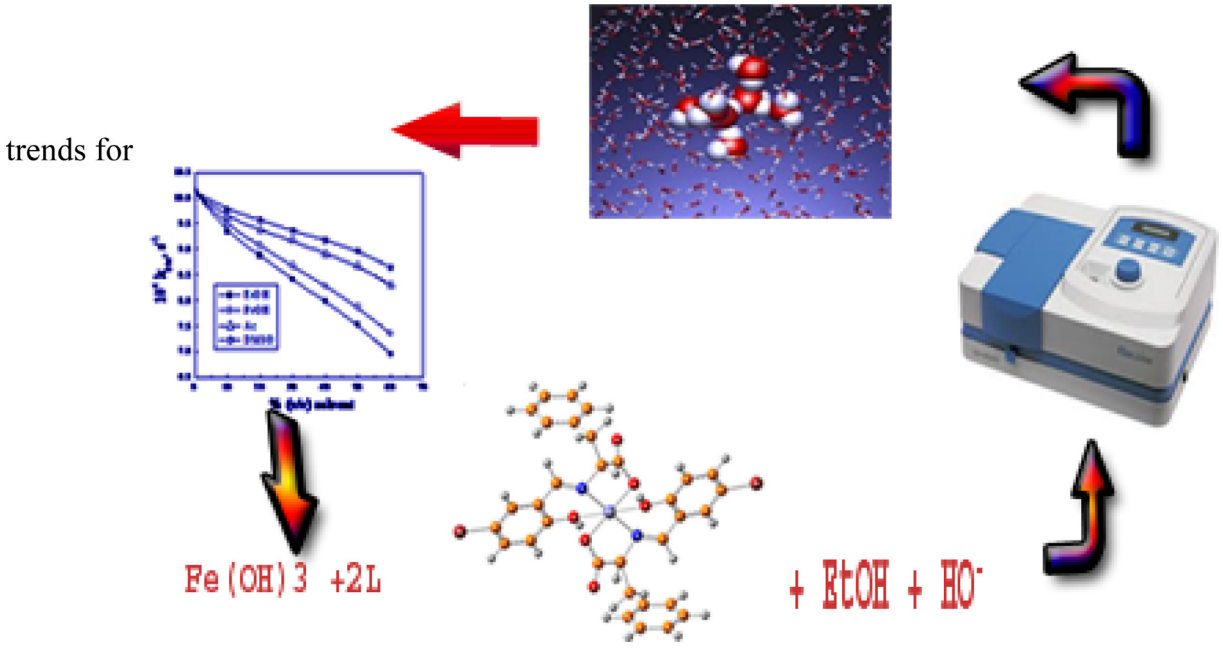

Scheme 2 Scheme of pathway for the base hydrolysis of the investigated complexes.

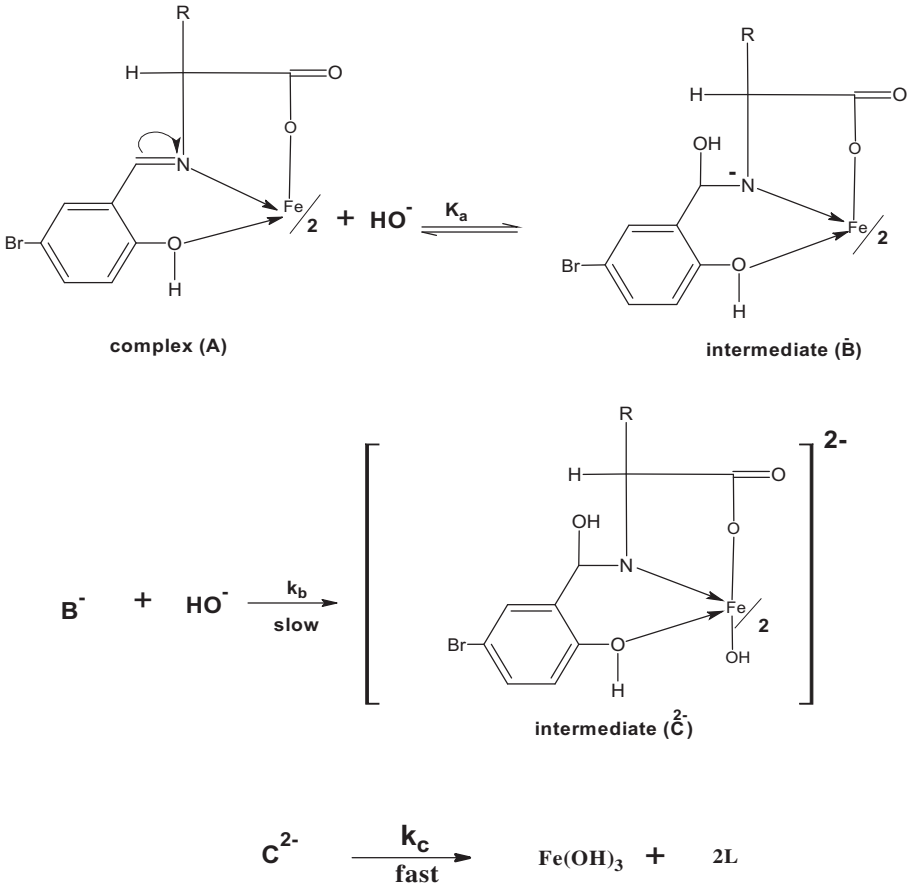

Scheme 3 The Suggested mechanism for the base hydrolysis reaction of the investigated complexes.

Table 1 Observed first order rate constant ($10^4\,k_{obs}$, s^{-1}) values for the base hydrolysis of the investigated Fe(II) bromosalicylidene amino acidate complexes in different ratios (v/v) of aqueous – organic solvent at $[OH^-] = 3.33 \times 10^{-3}$ mol dm^{-3}, [complex] $= 1.0 \times 10^{-4}$ mol dm^{-3}, $I = 0.01$ mol dm^{-3} and 298 K.

Complex	%						
	Solvent	0	10	20	30	40	50	60
bsali	EtOH	7.19	6.34	5.89	5.47	5.05	4.61	4.03
	PrOH		6.47	6.07	5.68	5.30	4.91	4.33
	Ac		6.65	6.39	6.14	5.87	5.62	5.25
	DMSO		6.86	6.61	6.40	6.18	5.97	5.62
bsasi	EtOH	10.13	9.33	8.87	8.41	7.97	7.52	6.95
	PrOH		9.47	9.07	8.66	8.28	7.86	7.35
	Ac		9.63	9.37	9.17	8.91	8.67	8.30
	DMSO		9.78	9.57	9.36	9.18	8.97	8.64
bshi	EtOH	9.08	8.23	7.78	7.35	6.93	6.48	5.91
	PrOH		8.38	8.02	7.61	7.19	6.82	6.31
	Ac		8.58	8.34	8.05	7.81	7.56	7.20
	DMSO		8.76	8.56	8.37	8.16	7.96	7.65
bsari	EtOH	5.57	4.73	4.26	3.84	3.39	2.95	2.41
	PrOH		4.89	4.48	4.10	3.72	3.31	2.80
	Ac		5.07	4.81	4.56	4.29	4.05	3.69
	DMSO		5.36	5.16	4.97	4.75	4.54	4.21

[a]Maximum error is 2%.

Table 2 Comparison between the reactivity of bsphali with Fe(II) hydroxynaphthylidene Schiff base amino acid complex (nphali) toward the attack of OH^- ion.

Complex	%						
	Solvent	0	10	20	30	40	50	60
bsphali	EtOH	8.22	7.41	6.96	6.52	6.09	5.63	5.04
	PrOH		7.57	7.17	6.79	6.38	6.01	5.51
	Ac		7.81	7.56	7.31	7.03	6.78	6.41
	DMSO		7.92	7.67	7.46	7.25	7.07	6.73
nhphali	EtOH	7.15	16.78	16.15	15.53	14.94	14.33	13.65
	PrOH		17.02	16.51	16.08	15.50	14.98	14.37
	Ac		17.28	16.88	16.49	16.08	15.65	15.07
	DMSO		17.42	17.13	16.81	16.50	16.21	15.79

Table 3 Second order rate constant values (10^2 k_2, mol^{-1} dm^3 s^{-1}) for the base hydrolysis reaction of the investigated Fe(II) bromosalicylidene Schiff base amino acid complexes in different ratios (v/v) of aqueous – organic solvent, [complex] = 1×10^{-4} mol $dm^{-3}$and $I = 0.01$ mol dm^{-3}.

Complex	%						
	Solvent	0	10	20	30	40	50	60
bsali	EtOH	17.42	16.26	15.71	15.11	14.52	13.87	13.31
	PrOH		16.51	15.94	15.57	14.98	14.57	13.98
	Ac		16.73	16.30	15.92	15.56	15.11	14.61
	DMSO		16.96	16.63	16.37	16.11	15.82	15.37
bsphali	EtOH	18.92	17.88	17.21	16.62	16.02	15.41	14.73
	PrOH		18.07	17.61	17.16	16.57	15.96	15.45
	Ac		18.33	17.98	17.51	17.16	16.73	16.14
	DMSO		18.52	18.21	17.87	17.61	17.33	16.86
bsasi	EtOH	20.63	19.51	18.97	18.42	17.81	17.21	16.62
	PrOH		19.62	19.25	18.71	18.33	17.91	17.18
	Ac		19.91	19.53	19.22	18.77	18.35	17.87
	DMSO		20.22	19.81	19.53	19.28	18.93	18.50
bshi	EtOH	19.52	18.33	17.82	17.38	16.78	16.21	15.56
	PrOH		18.48	18.10	17.65	17.21	16.8	16.23
	Ac		18.69	18.32	17.87	17.63	17.15	16.6
	DMSO		19.10	18.83	18.39	18.16	17.85	17.38
bsari	EtOH	16.21	14.91	14.06	13.78	13.24	12.70	11.94
	PrOH		15.17	14.68	14.17	13.75	13.18	12.61
	Ac		15.45	15.11	14.76	14.25	13.86	13.47
	DMSO		15.79	15.37	15.14	14.83	14.61	14.24

[a]Maximum error is 2%.

Mahmoud et al. (1986). The second hydroxide ion slowly attacks the central iron atom in the intermediate B^{2-} (cf. The following mechanism) followed by degradation of the complex.

The values of observed rate constants for the base hydrolysis reaction of bsphali were compared with the corresponding derivative nphali from previous publication (Abdel-Rahman et al., 2013) (cf. Table 2). The data show that the effect of function group on the reactivity trends of the prepared complexes toward the attack of OH^- ion on them. It is observed that the reactivity of bsphali toward the base hydrolysis is more than the corresponding nphali. This is because the inductive effect of bromide atom in bsphali is more than the phenyl ring in nphali.

From the comparison between the values of second-order rate constant (k_2) of the base hydrolysis of the studied complexes (cf. Table 3), it was found that the values of k_2 are correlated with the effect of side chain substituent R in the structure of the complexes under investigation. The order of reactivity of the prepared bromosalicylidene complexes toward the hydroxide attack is increased in the sequence: bsari < bsali < bsphali < bshi < bsasi. This may be rationalized to the inductive effect of the substituent. This may be due to the electron withdrawing properties of carboxylic group more in bsasi than imidazole ring in bshi and phenyl ring in bsphali. Where in bsari, the presence of a guanidine group which is strong electron donating group makes its reactivity toward OH^- low.

The solubility of the prepared complexes was measured in aqueous solution, aqueous-organic solvents such as ethanol, propanol, acetone and dimethyl sulfoxide (cf. Table 4). The transfer chemical potentials for an uncharged compound are generally derived from solubility measurement on the assumption that the ratio of mean activity values co-efficient in the aqueous and aqueous-organic mixtures was in all cases unity

Table 4 Solubility (mol dm^{-3}) values of the prepared complexes in different ratios (v/v) of EtOH at 298 K.

Solvent	Complex	Solubility10^4 mol dm^{-3}			
		0	20	40	60
EtOH[a]	bsali	1.89	4.97	11.30	16.80
	bsphali	0.25	0.90	5.59	9.76
	bsasi	2.10	4.12	8.43	15.18
	bshi	0.41	1.25	2.75	7.50
	bsari	1.40	3.92	8.92	14.50
PrOH	bsali	1.89	5.17	11.70	18.75
	bsphali	0.25	1.15	7.43	10.86
	bsasi	2.10	4.73	8.61	17.08
	bshi	0.41	1.41	3.11	8.23
	bsari	1.40	4.12	9.74	16.44
Acetone	bsali	1.89	5.44	12.13	20.27
	bsphali	0.25	1.48	8.35	11.67
	bsasi	2.10	5.22	9.13	18.11
	bshi	0.41	1.65	3.72	8.85
	bsari	1.40	4.52	10.20	17.15
DMSO[a]	bsali	1.89	7.75	14.42	22.51
	bsphali	0.25	3.75	10.61	13.96
	bsasi	2.10	7.55	11.46	20.39
	bshi	0.41	3.91	5.89	11.15
	bsari	1.40	6.85	12.34	19.40

[a] From Ref. Abdel-Rahman, L.H., El-Khatib, R.M., Nassr, L. A.E., Abu-Dief, A.M. Arab. J. Chem. Acceptedmanuscript, 2013. Available from: http://dx.doi.org/10.1016/j.arabjc.2013.07.010.

Table 5 Initial state (IS)-Transition state (TS) analysis of solvent effects on reactivity trends for the base hydrolysis of (bsali) in different ratios (v/v) of solvent at 298 K.

Solvent	Solvent %	$\delta_m\mu^0$ (bsali) kJ mol^{-1}	$\delta_m\mu^0$ (OH^-) kJ mol^{-1}	$\delta_m\mu^0$ (IS) kJ mol^{-1}	$\delta_m\Delta G^{\#}$ kJ mol^{-1}	$\delta_m\mu^0$ (TS) kJ mol^{-1}
EtOH	20	−2.42	1.15	−1.15	−0.26	−1.41
	40	−4.43	4.40	−0.03	−0.45	−0.48
	60	−5.42	9.52	4.1	−0.67	3.43
Acetone	20	−2.62	4.98	2.36	−0.16	2.20
	40	−4.61	11.79	7.18	−0.28	6.90
	60	−5.88	21.03	15.15	−0.44	14.71
DMSO	20	−3.50	6.20	2.7	−0.12	2.58
	40	−5.04	14.56	9.52	−0.19	9.33
	60	−6.14	29.39	23.25	−0.31	22.94

Table 6 Initial state (IS)-Transition state (TS) analysis of solvent effects on reactivity trends for the base hydrolysis of bsphali in different ratios (v/v) of solvent at 298 K.

Solvent	Solvent %	$\delta_m\mu^0$ (bsphali) kJ mol^{-1}	$\delta_m\mu^0$ (OH^-) kJ mol^{-1}	$\delta_m\mu^0$ (IS) kJ mol^{-1}	$\delta_m\Delta G^{\#}$ kJ mol^{-1}	$\delta_m\mu^0$ (TS) kJ mol^{-1}
EtOH	20	−3.16	1.15	−2.01	−0.23	−2.24
	40	−7.70	4.40	−3.30	−0.41	−3.71
	60	−9.05	9.52	0.47	−0.62	−0.15
Acetone	20	−4.31	4.98	0.67	−0.13	0.54
	40	−8.70	11.79	3.09	−0.24	2.85
	60	−9.53	21.03	11.5	−0.39	11.11
DMSO	20	−6.71	6.20	−0.51	−0.095	−0.61
	40	−9.29	14.56	5.27	−0.18	5.09
	60	−9.97	29.39	19.42	−0.28	19.14

(Bähr and Thämlitz, 1955) according to the following thermodynamic equation:

$$\delta_m\mu^{\theta}(\text{compound}) = -RT\ln\left(\frac{S_S}{S_W}\right) \quad (2)$$

where S_S and S_W refer to the solubility in water-solvent mixture and aqueous solution, respectively. Thus, the values of $\delta_m\mu^{\theta}$, the transfer chemical potentials of the investigated complexes from water to water-organic binary mixtures are calculated and cited in Tables 5–9 from solubility

Table 7 Initial state (IS)-Transition state (TS) analysis of solvent effects on reactivity trends for the base hydrolysis of bsasi in different ratios (v/v) of solvent at 298 K.

Solvent	Solvent %	$\delta_m\mu^0$ (bsasi) kJ mol^{-1}	$\delta_m\mu^0$ (OH^-) kJ mol^{-1}	$_m\mu^0$ (IS)δ kJ mol^{-1}	$\delta_m\Delta G^{\#}$ kJ mol^{-1}	$\delta_m\mu^0$ (TS) kJ mol^{-1}
EtOH	20	−1.67	1.15	−0.52	−0.21	−0.73
	40	−3.45	4.40	0.95	−0.36	0.59
	60	−4.90	9.52	4.62	−0.54	4.08
Acetone	20	−2.26	4.98	2.72	−0.14	2.58
	40	−3.64	11.79	8.15	−0.23	7.92
	60	−5.34	21.03	15.69	−0.36	15.33
DMSO	20	−3.17	6.20	3.03	−0.10	2.93
	40	−4.21	14.56	10.35	−0.17	10.18
	60	−5.64	29.39	23.75	−0.27	23.48

Table 8 Initial state (IS)-Transition state (TS) analysis of solvent effects on reactivity trends for the base hydrolysis of (bshi) in different ratios (v/v) of solvent at 298 K.

Solvent	Solvent %	$\delta_m\mu^0$ (bshi) kJ mol^{-1}	$\delta_m\mu^0$ (OH^-) kJ mol^{-1}	$\delta_m\mu^0$ (IS) kJ mol^{-1}	$\delta_m\Delta G^{\#}$ kJ mol^{-1}	$\delta_m\mu^0$ (TS) kJ mol^{-1}
EtOH	20	−2.76	1.15	−1.61	−0.23	−1.84
	40	−4.72	4.40	−0.32	−0.38	−0.7
	60	−7.21	9.52	2.31	−0.56	1.75
Acetone	20	−3.45	4.98	1.53	−0.16	1.37
	40	−5.47	11.79	6.32	−0.25	6.07
	60	−7.62	21.03	13.41	−0.4	13.01
DMSO	20	−5.59	6.20	0.61	−0.09	0.52
	40	−6.61	14.56	7.95	−0.19	7.76
	60	−8.19	29.39	21.2	−0.29	20.91

Table 9 Initial state (IS)-Transition state (TS) analysis of solvent effects on reactivity trends for the base hydrolysis of bsari in different ratios (v/v) of EtOH at 298 K.

Solvent	Solvent %	$\delta_m\mu^0$ (bsari) kJ mol^{-1}	$\delta_m\mu^0$ (OH^-) kJ mol^{-1}	$\delta_m\mu^0$ (IS) kJ mol^{-1}	$\delta_m\Delta G^{\#}$ kJ mol^{-1}	$\delta_m\mu^0$ (TS) kJ mol^{-1}
EtOH	20	−2.55	1.15	−1.40	−0.35	−1.75
	40	−4.57	4.40	−0.17	−0.5	−0.67
	60	−5.80	9.52	3.72	−0.76	2.96
Acetone	20	−2.91	4.98	2.07	−0.17	1.90
	40	−4.92	11.79	6.87	−0.32	6.55
	60	−6.21	21.03	14.82	−0.46	14.36
DMSO	20	−5.59	6.20	0.61	−0.09	0.52
	40	−6.61	14.56	7.95	−0.19	7.76
	60	−8.19	29.39	21.2	−0.29	20.91

measurements in different aqueous solution and water–solvent mixtures according to Eq. (2).

The hydrophobicity of the investigated Fe(II) Schiff base amino acid complexes can be rationalized to the low solubility of the investigated complexes in aqueous medium (cf. Table 4). Moreover, the results of negative values transfer chemical potentials of none charged the investigated Fe(II) Schiff base amino acid complexes (cf. Tables 5–9) can mainly be ascribed to the hydrophobic nature of the investigated complexes. It is observed that the hydrophobicity of the investigated complexes leads to an increase in the stabilization of them with increasing solvent percent. The order of the hydrophobicity increases in the following order:

bsasi < bsali < bsari < bshi < bsphali

Thus the results show preferential solvation by the solvent as molecule size increases.

The effect of co-organic solvent on the reactivity has been investigated in the presence of ethanol, propanol, acetone and dimethyl sulfoxide and the observed first-order rate constant values (k_{obs}) for the base hydrolysis were evaluated and reported in Table 4 and Figs. 1 and 2. The increase of the added co-solvent % exhibits a general decrease of the rate constants of the base hydrolysis of the examined complexes. This reactivity trend is attributed to the opposed effects of the extensive destabilization or to the salting out of the OH^- ion (Abu-Gharib et al., 2011; Abu-Gharib et al., 2017; El-Khatib and Nassr, 2007). Furthermore, the high delocalization of charge within Fe(II) azomethine complex promotes interaction with localized dispersion centers in nearby solvent molecules (Abu-Gharib et al., 2011, 2017; Shaker and Nassr, 2002). Thus, the destabilization of OH^- ions and conversely the stabilization of the complex in the presence of increasing amounts of co-solvent in the reaction aqueous medium, as evidenced from the remarkably increased solubility on going from the

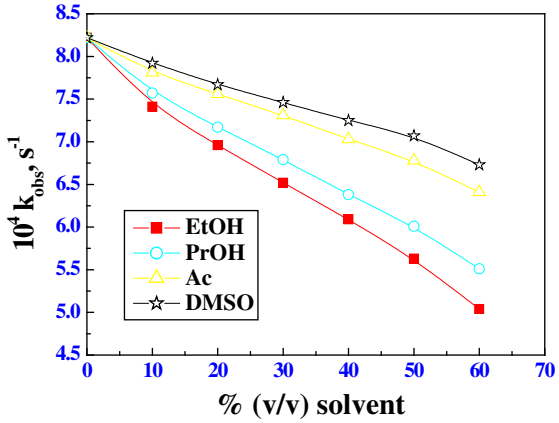

Figure 1 Plots of the observed first-order rate constant values for the base hydrolysis of bsphali complex in different ratios (v/v) of solvent at [bsphali] = 1.0×10^{-4} mol dm^{-3}, [OH$^-$] = 3.33×10^{-3} and 298 K.

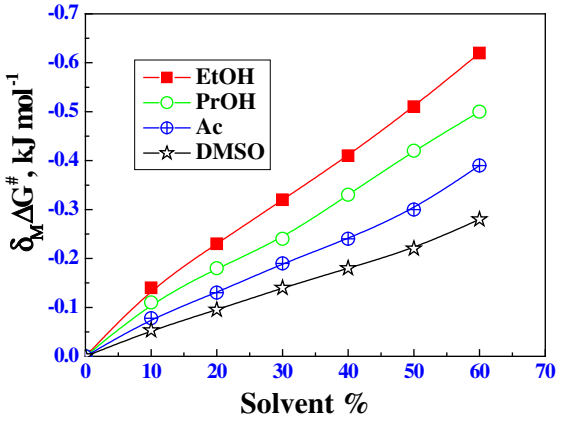

Figure 2 Plots of the change in the activation barrier ($\delta_m \Delta G^{\#}$) for the base hydrolysis of bsphali complex in different ratios (v/v) of solvent at 298 K.

aqueous to 60% (v/v) co-solvent solution as shown in Tables 4 and 5 reduce the opportunity of the reactants to combine together to afford the activated complex and thus reduces the reaction rate. The effective density of dispersion centers in solvent molecules increases in the order H_2O < DMSO < acetone < propanol < ethanol. Thus this type of interaction is expected to be weak as the mole fraction of water increases. Thus, in turn, leads to destabilize the azomethine compound in the same direction.

In accordance with the proposed mechanism in all of the systems, the transition state is more hydrophilic than the initial state, because of the more ionic character of the former. In general, the transition state would be less stabilized by solvation with increasing amounts of the co-solvent compared with the initial state. This effect, combined with the destabilization of the convenient hydrophilic simple OH^- ion, would lead to an enhanced reaction rate due to the greater opportunity of the destabilized reactants to bind. However, this is not the case for the recently observed reactivity trends in most complexes investigated. This paradox in the reactivity trends would be intuitively attributable to competition between the opposing effects of the stabilization by dispersion or solvation of the particular complex, on one hand, and the destabilization of OH^- ions in co-solvents, on the other hand. If compensation between these two effects occurred, there should be small effects on reactivity on adding organic co-solvents to the aqueous reaction.

Tables 5–9 and Figs. 2 and 3 indicate that the values of activation energy barrier ($\delta_m \Delta G^{\#}$) at different ratios of co-solvent increase with increase in ethanol, propanol, acetone and dimethyl sulfoxide %. These trends match with the decrease in the values of k_2 as co-solvent % increases.

3.2. Initial state-transition state analysis for the investigated complexes in water-solvent mixtures

Solvent effects on the rate constants reflect solvation changes on the initial and transition states as these are transferred from water into mixed aqueous methanol or aqueous acetone media. If solvent effects on the initial state can be established from thermodynamic data (solubility data), then solvent effects on

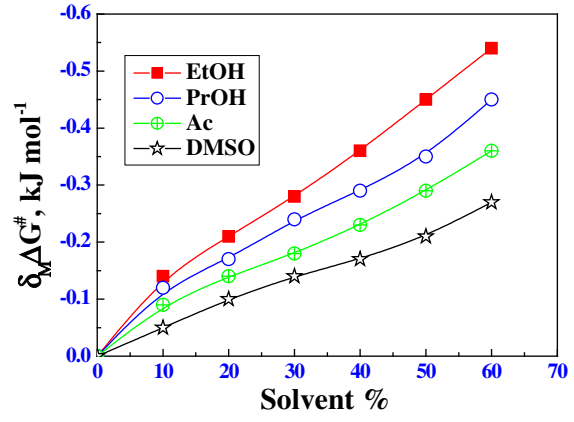

Figure 3 Plots of the change in the activation barrier ($\delta_m \Delta G^{\#}$) for the base hydrolysis of bsasi complex in different ratios (v/v) of solvent at 298 K.

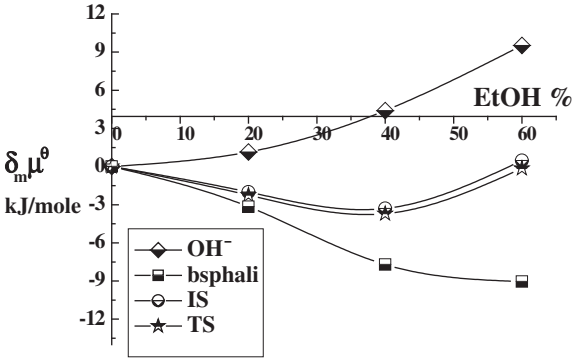

Figure 4 Plots of the initial state (IS) and transition state (TS) for the base hydrolysis of bsphali complex in different ratios (v/v) of EtOH at 298 K.

the transition state can be calculated from initial state and kinetic data assuming constancy of mechanism and validity of transition state theory. The free energies of activation and

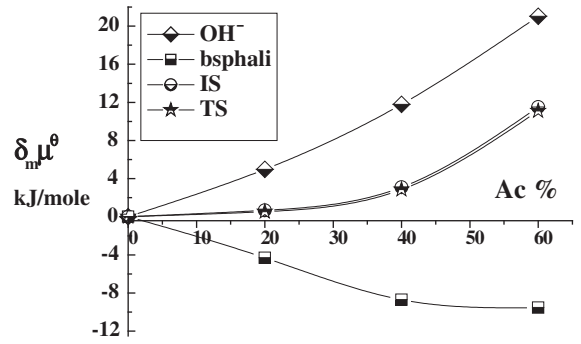

Figure 5 Plots of the initial state (IS) and transition state (TS) for the base hydrolysis of bsphali complex in different ratios (v/v) of Ac at 298 K.

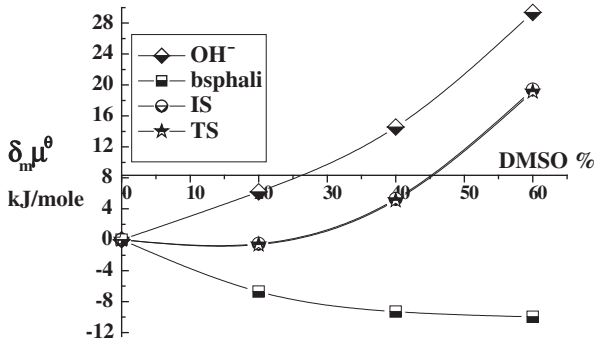

Figure 6 Plots of the initial state (IS) and transition state (TS) for the base hydrolysis of bsphali complex in different ratios (v/v) of DMSO at 298 K.

transfer chemical potentials are now used in our analysis of reactivity trends with changing solvent composition into initial state and transition state components, i.e., combination of kinetic data, solubility data and transfer chemical potentials yield the effect of solvent on the transition state according to equation (Abu-Gharib et al., 2011 ,2017; Blandamer et al., 1986; El-Khatib, 2002):

$$\delta_m\Delta G^{\#}(c-\text{scale};P;T) = \{\delta_m\mu^{\#}(c-\text{scale};P;T) - \delta_m\mu^{\theta}(OH^-,c-\text{scale};P;T) - \delta_m\mu^{\theta}(\text{compound};c-\text{scale};P;T)\} \quad (3)$$

In the present work we use the concentration scale, the pressure P is ambient and T is 298 K. Transfer chemical potentials for OH^- in ethanol, acetone and dimethylsulfoxide are obtained from previous publications (Blandamer et al., 1986; Marcus, 2007; Abu-Gharib et al., 2011, 2017). Details of the initial state-transition state analyses of reactivity trends according to Abraham's assumption (Ph_4P^+, Ph_4As^+) = (Ph_4B^-) are set out in Tables 5–9 and illustrated in Figs. 4–6. The results in Tables 5–9 and Figs. 4–6 show that the investigated complexes are stabilized and the hydroxide ion is significantly destabilized on transfer from water to 60% solvent resulting in an overall decrease in stabilization of the initial state (IS). On the other hand the transition state (TS) is destabilized on going from water to 60% ethanol. Thus, the observed decrease in the rate constant can be attributed to high destabilization of the initial state, rather than to less stabilization of the transition state i.e. the dominant effect of (IS) on the rate constant of the base hydrolysis of the investigated complexes as the co solvent % increases.

4. Conclusion

Base catalyzed hydrolysis of some Fe(II) Schiff base amino acid complexes follows a rate law with $k_{obs} = k_2[OH^-]$. The decrease in the rate constants of the investigated complexes as the proportion of solvent increases is due to the destabilization of OH^- ion. The values of rate constants (k_{obs} and k_2) decrease in the following order water > DMSO acetone > propanol > ethanol with increasing the solvent content. The dominant effect on the rate constant of the base hydrolysis of the investigated complexes as the co-solvent percent increases is the initial state.

References

Abdel-Rahman, L.H., El-Khatib, R.M., Nassr, L.A.E., Abu-Dief, A.M., 2013. J. Saudi Chem. Soc., accepted manuscript, http://dx.doi.org/10.1016/j.jscs.2013.11.004.
Abdel-Rahman, L.H., El-Khatib, R.M., Nassr, L.A.E., Abu-Dief, A.M., Lashin, F.E., 2013. Spectrochim. Acta 111, 266.
Abdel-Rahman, L.H., El-Khatib, R.M., Nassr, L.A.E., Abu-Dief, A.M., Ismael, M., Seleem, A.A., 2014. Spectrochim. Acta 117, 366-37.
Abu-Gharib, E.A., EL-Khatib, R.M., Nassr, L.A.E., Abu-Dief, A.M., 2011. Z. Phys. Chem. 225 (1).
Abu-Gharib, E.A., EL-Khatib, R.M., Nassr, L.A.E., Abu-Dief, A.M., 2017. Arab. J. Chem. 10, S988–S995.
Bähr, G., Döge, H.G., 1957. Anorg Allgem. Chem. 292, 119.
Bähr, G., Thämlitz, H.Z., 1955. Anorg. Allgem. Chem. 282, 3.
Blandamer, M.J., Burgess, J., Clark, B., Duce, P.P., Haken, A.W., Gosal, N., Guradado, P., Sanches, F., Hubard, C.D., Abu-Gharib, E.A.J., 1986. Chem. Soc. Faraday Trans. 1 (82), 1471.
Blandamer, M.J., Briggs, B., Burgess, J., Elvidge, D., Clark, B., Guardado, P.A., Hakin, W., Sanchez, F., Radulovic, S., Hubbard, C.D.J., 1988. Chem. Soc. Faraday Trans. 1 (84), 2703.
Blandamer, M.J., Burgess, J., Fawcett, J., Guardado, P., Hubbard, C.D., Nuttall, S., Prouse, L.J.S., Radulovic, S., Russell, D.R., 1992. Am. Chem. Soc. Inorg. Chem. 31 (8), 1383.
Burgess, J., Pelizzetti, E., 1988. Gazz. Chim. Ital. 118, 803.
Burgess, J., Pelizzetti, E., 1992. Prog. React. Kinet. 17, 1.
Canali, L., Sherrington, D.C., 1999. Chem. Soc. Rev. 28, 85.
El-Khatib, R.M., 2002. J. Indian Chem. Soc. 41A (1).
El-Khatib, R.M., Nassr, L.A.E., 2007. Spectrochim. Acta A 67, 643.
El-Said, A.I., Zidan, A.S.A., El-Meligy, M.S., Aly, A.A.M., Mohammed, O.F., 2001. Transit. Met. Chem. 26, 13.
Mahmoud, R.M., Hamed, M.A., Shaker, A.M., 1986. J. Solution Chem. 15, 9.
Marcus, Y., 2007. Chem. Rev. 107, 3880.
Milde, S.P., Blandamer, M.J., Burgess, J., Engberts, J.B.F.N., Galena, S.A., Hubbard, C.D., 1999. J. Phys. Org. Chem. 12, 227.
Nath, M., Yadov, R., 1997. Bull. Chem. Soc. Jpn. 70, 131.
Shaker, A., Nassr, L.A.E., 2002. Int. J. Chem. Kinet. 34, 595.
Sharma, P.K., Dubey, S.N., 1994. Indian J. Chem 33A, 1113.
Wang, Z.M., Lin, H.K., Zhu, S.R., Liu, T.F., Chen, Y.T., 2002. J. Inorg. Biochem. 89, 97.
Wang, M.Z., Meng, Z.X., Liu, B.L., Cai, G.L., Zhang, C.L., Wang, X.Y., 2005. Inorg. Chem. Commun. 8 (4), 368.
Yamagishi, A., 1986. Inorg. Chem. 25, 55.